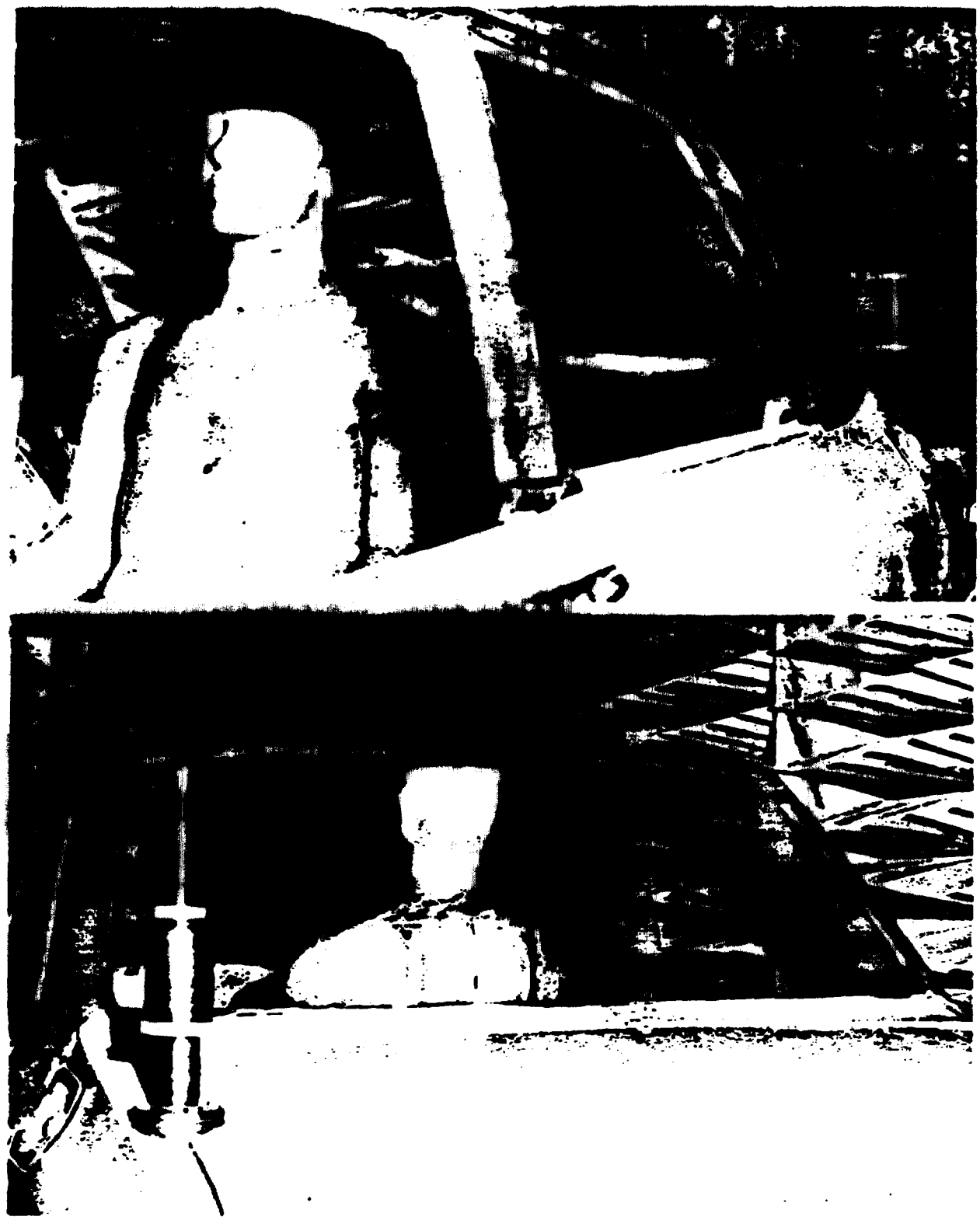

Fig. 22. Sitting man model in back seat of automobile exposed to trunk-mounted antenna.

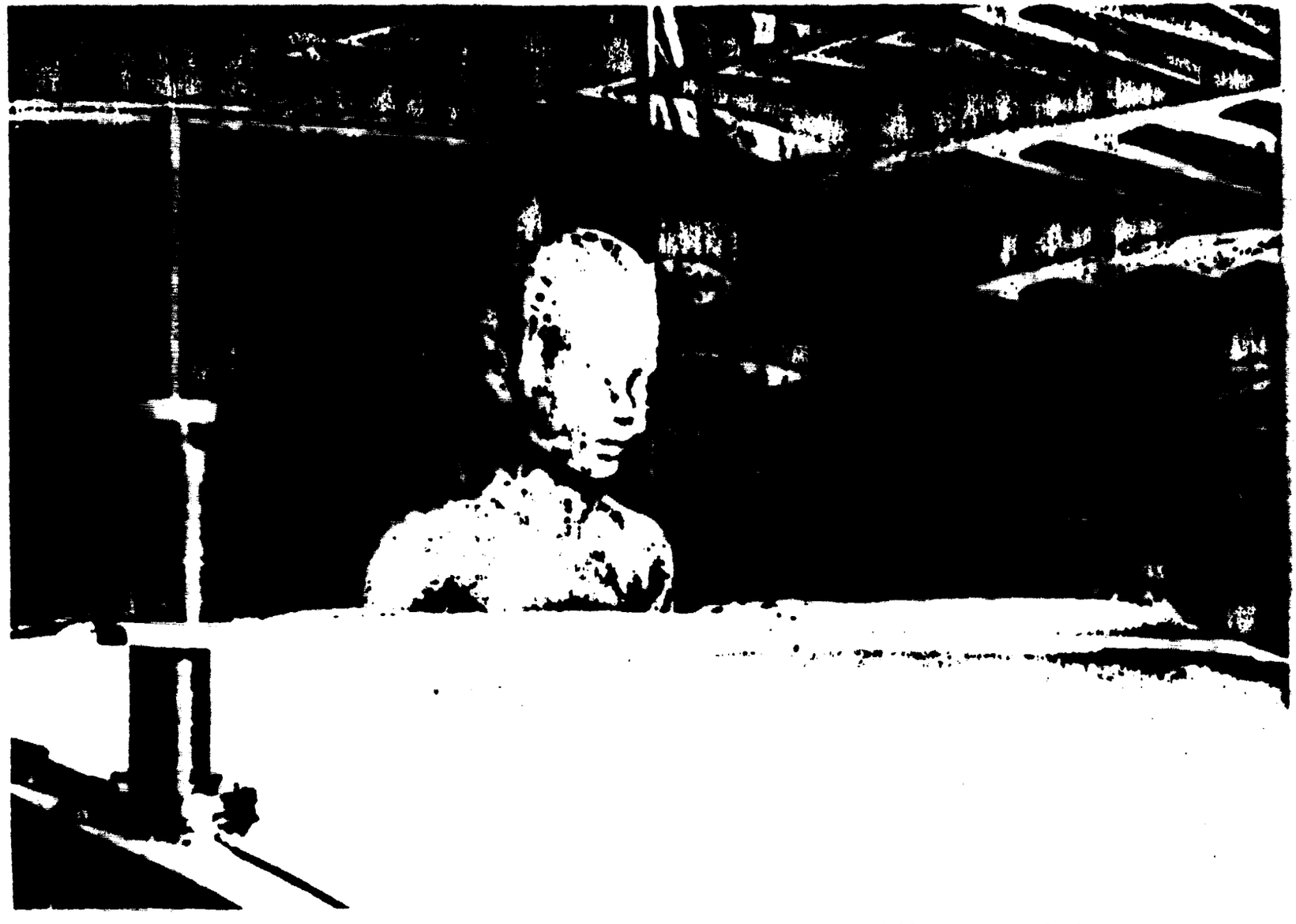

Fig. 23. Kneeling child model interior of automobile exposed to trunk-mounted antenna.

Measurement of Electromagnetic Fields in and out of Automobile

In order to characterize the exposure field conditions, we made a number of electromagnetic fields measurements using the EDM-1C energy-density meter. Measurements outside of the automobile were made at the sagittal plane of the model exposed to both the roof- and trunk-mounted antennas. In Fig. 24 is illustrated the position of the meter probe during the measurements. We placed absorbing material between the meter and the antenna to prevent the fields from being perturbed and moved the probe in 5-cm increments in vertical and horizontal directions. The fields inside the automobile were measured in a three-dimensional space as shown in Fig. 25. Measurements were made every 10 cm in three dimensions. Absorbing material was also placed between the meter and the probe. Measurements were made under low power conditions well below the ANSI C95.1-1982 exposure standard.

Measurement of SAR

Thermography

The thermographic method provides the most efficient way for establishing SAR over a two-dimensional internal plane within the exposed model. This method, described in detail elsewhere by Guy (1971) and Guy et al. (1976b), is valid for both far- and near-zone fields and involves the use of a thermographic camera for recording the temperature distributions produced by energy absorption in phantom models after exposure to radiation fields. In Figs. 26 and 27 is illustrated the methodology of using thermography. As shown in Fig. 26, the model was first disassembled along a plane where SAR was to be determined. For this instance, the horizontal plane through the eyes of the child model was exposed with the head near the transmitting antenna. Before exposure the model was disassembled, and a thermograph temperature scan was made of the plane as shown in Fig. 27. The model was then reassembled, exposed for a short time to high power density of known level, and then again disassembled, and another

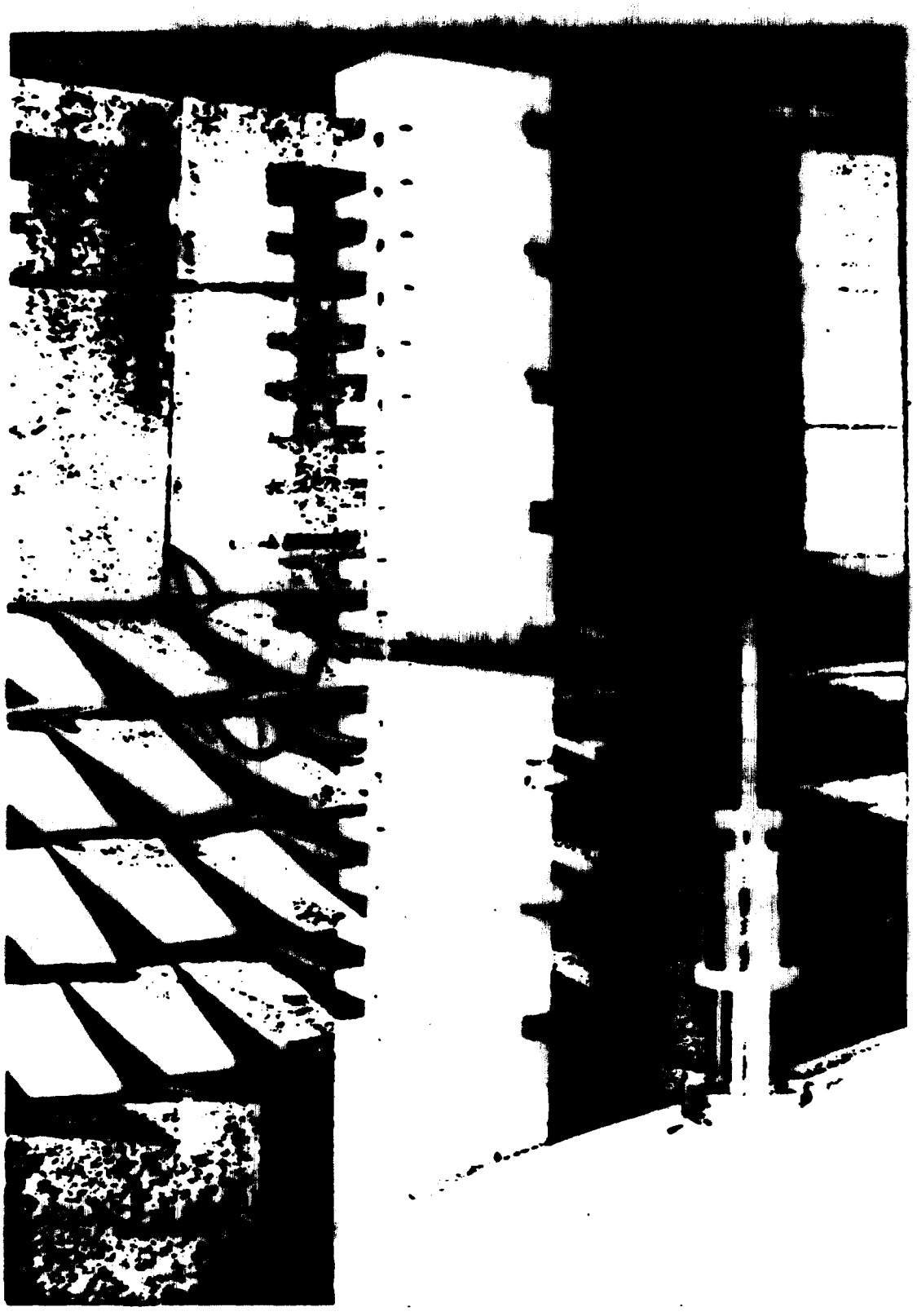

Fig. 24. Measurement of power-density pattern in vicinity of trunk-mounted antenna with EDM-1C survey meter.

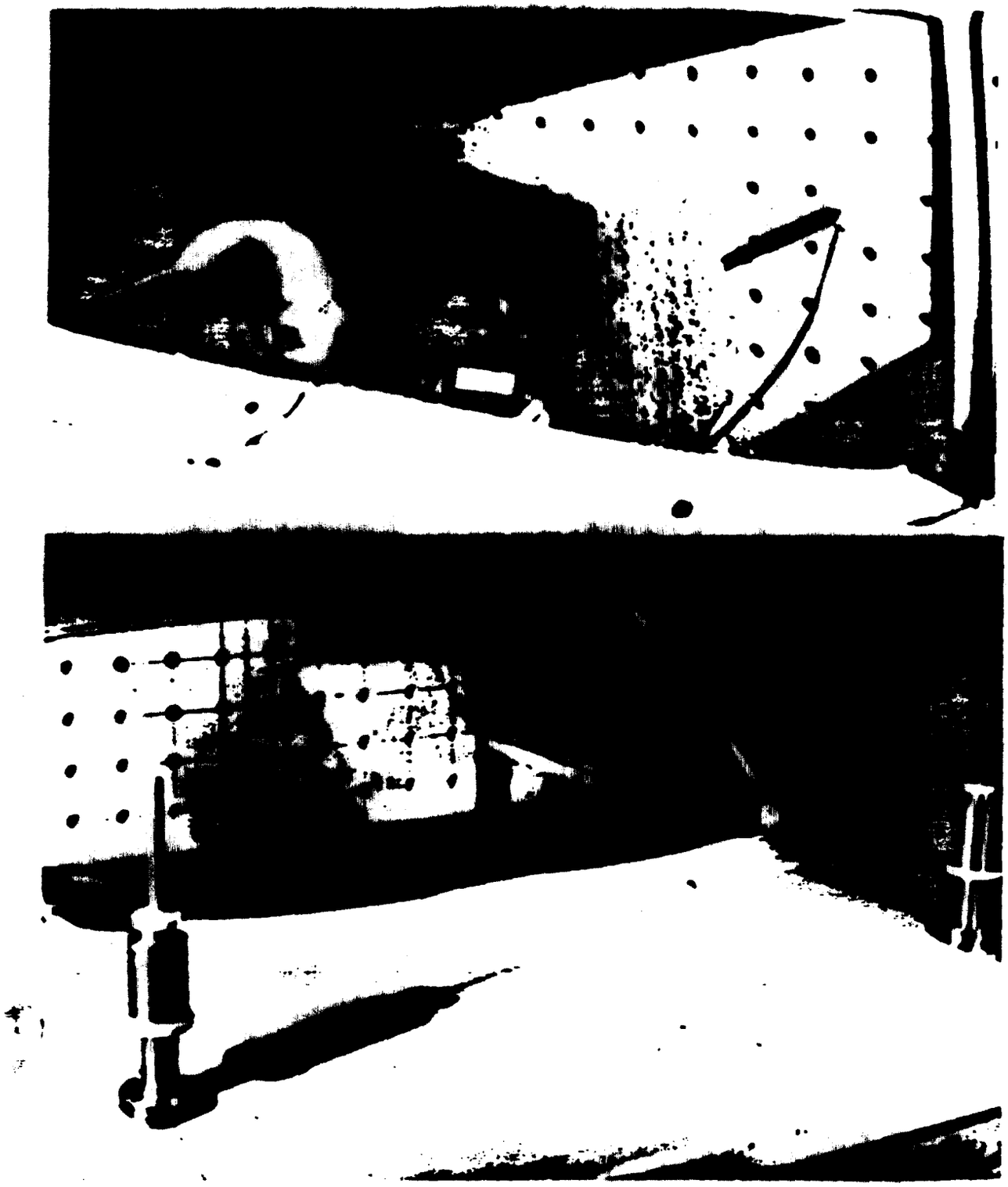

Fig. 25. Arrangement of EDM-1C meter probe for measuring power density pattern in interior of automobile due to emission from trunk-mounted antenna.

Fig. 26. Separation along orbital plane of phantom child model exposed to roof-mounted antenna.

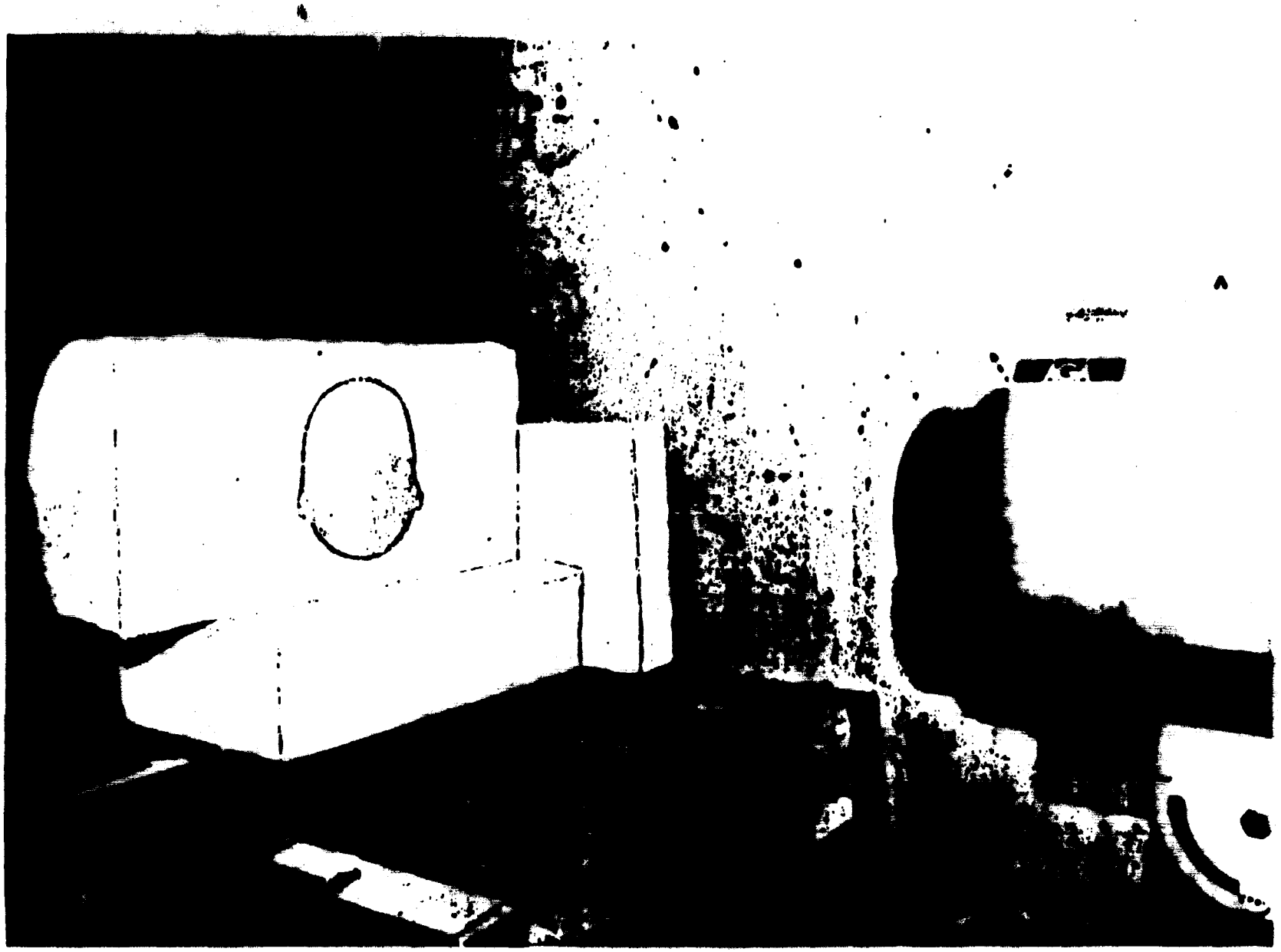

Fig. 27. Thermograph scanning orbital plane of phantom child model.

thermographic scan was made. Figs. 12 and 16 illustrate the models oriented for sagittal-plane thermographic scans. In the case of the child kneeling in back of the car, looking out the back window as shown in Fig. 23, the model was separated as shown in Fig. 28 to reveal the absorption in the sagittal plane of the head.

The standard thermographic method previously reported was used for determination of the SAR in the foam woman and child models exposed to the roof-mounted antennas. A two-dimensional gray-scale scan was immediately photographed after exposure of the model, and single B-scans with amplitude proportional to temperature were made before and after exposure. The two B-scans were photographed sequentially on the same film so that they were superimposed one upon the other as shown in Figs. 47-54 in the Results section.

For later thermographic work with the trunk-mounted antenna, however, an improved thermographic technique was employed with digital recording and interactive-computer analysis. This newer method is described in detail in Appendix A. In general, whole-body thermograms were first taken over the bisected models for identification of regions of maximum SAR. Then a second series of thermographs were taken, in which the camera was moved closer to the object for better resolution of the regions where high SAR occurred.

Vitek 101 Temperature Probe

Since the thermographic measurements provided only the SAR at the bisected surfaces, the SARs at other locations of the model had to be measured by other means. Four Vitek 101 temperature probes were used to measure the rate of temperature rise at four locations simultaneously. To minimize heat diffusion, we applied the same high-power exposure technique that was used in the thermographic method over a period of about 1 min. The rate of temperature rise was recorded. In both man and woman models, the SARs at the heart, kidney, liver, and stomach region were measured (Fig. 29). Since the breasts of the woman model were very close to the tip

Fig. 28. Method of separating parts of kneeling child model for determination of SAR in sagittal plane of head.

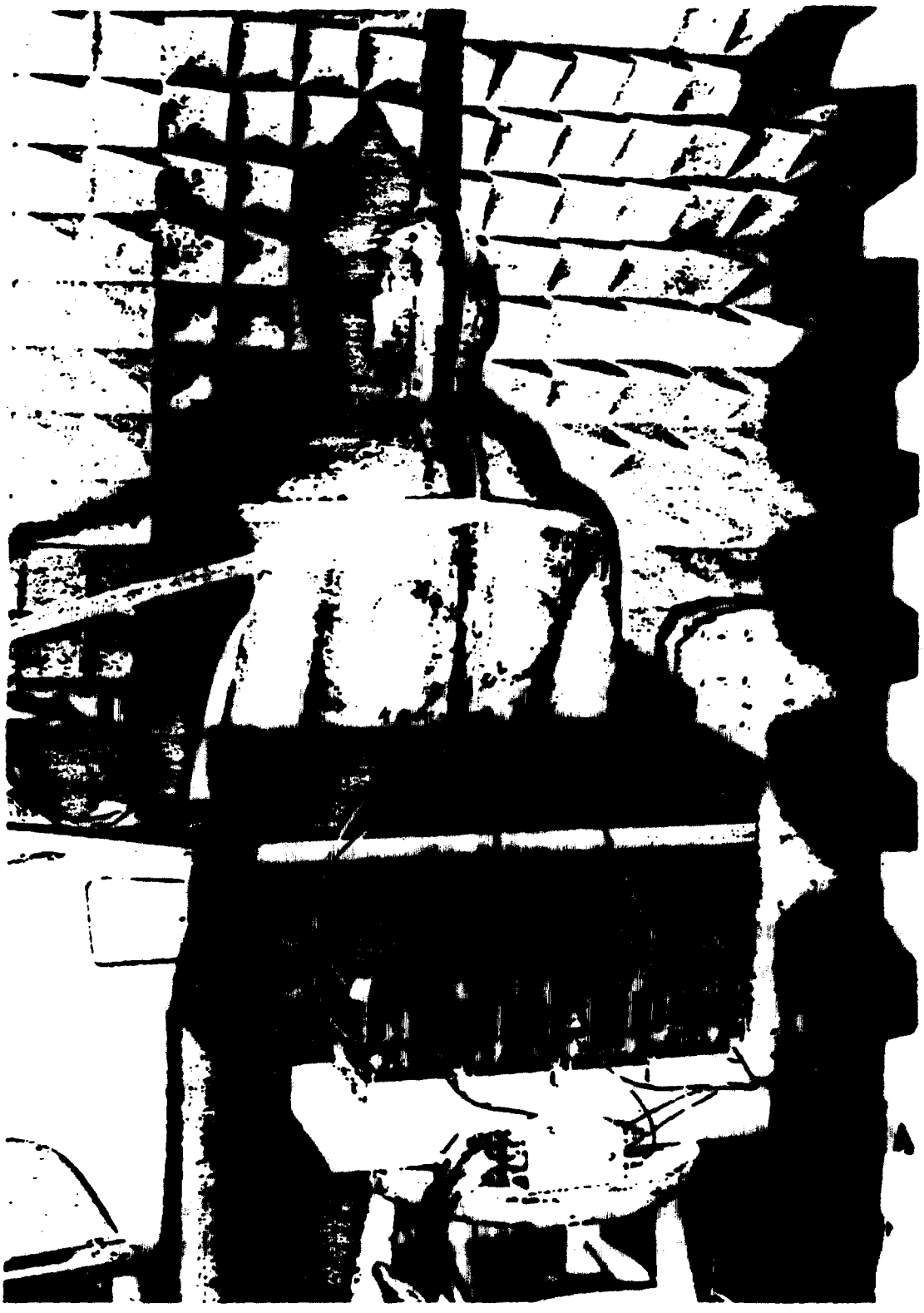

Fig. 29. Four Vitek 101 temperature probes for measuring simultaneously SAR in man model at four locations.

of the trunk-mounted antenna, the SAR in the center line of the breasts and 2.8 cm below the center line were also measured. For the child model, regions in the eyes, brain, and mouth were measured.

Electric-Field Probe

In order to measure SAR levels in models exposed to the weaker fields within the automobile, we made an attempt to measure the internal fields using a Narda, implantable electric-field probe. Because of the relative absence of sensitivity of the probe, however, the method was abandoned in favor of developing a more sensitive probe.

It was decided to use a Schottky diode of the type used for standard survey meters as a sensing element for the electric field. Initially, the leads of the diode were used as the antenna, and the diode itself was used to rectify the radio-frequency energy. High-resistance, small-diameter wires were used to carry the resulting DC signal back to a meter. Much greater sensitivity was obtained by modulation of the RF-source at 1,000 Hz and use of a Hewlett-Packard 415E standing wave detector for sensing the 1,000-Hz signal from the diode.

It was found, however, that the leads in the solid-state junction within the glass bead of the diode and the connected high-resistance leads formed a loop that was also sensitive to magnetic field. This was eliminated by encapsulation of the diode in a conducting, bisecting pillbox (shown in Figs. 30 and 31) such that the bisected pillbox formed the poles of the receiving dipole and at the same time shielded the loop formed by the high-resistance wire connections, preventing any induced voltages caused by magnetic fields.

The diode used was an Aertech AZS810. The high-resistance, twisted-pair, .001"-diameter, .7-ohm-per-foot, nylon-coated resistance wire was protected from strain and mechanical damage by a 1/4", 30-cm-long acrylic tube. The high-resistance leads continued beyond the acrylic tube through a 90-cm-long, flexible Tygon plastic tubing. The twisted pair of

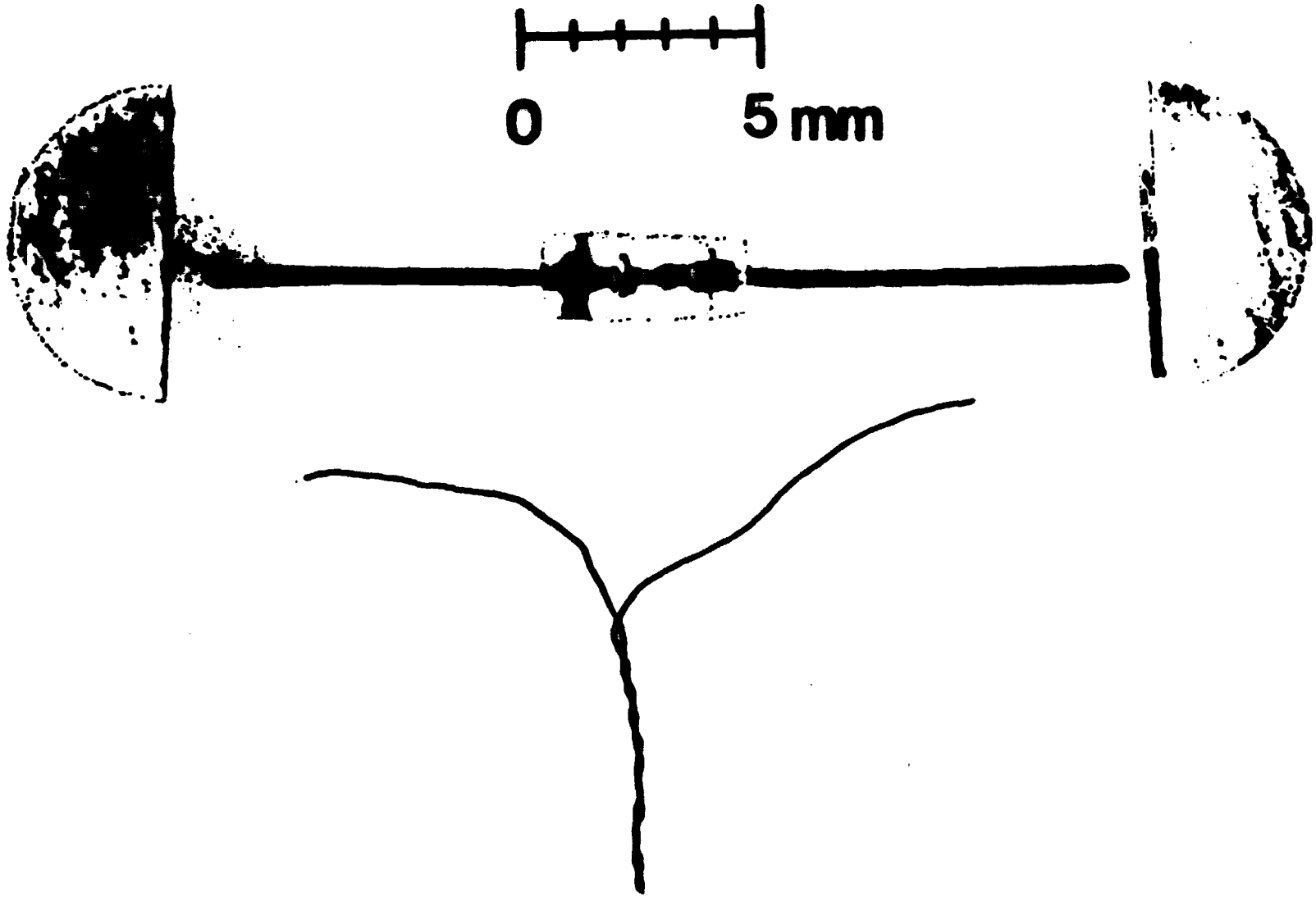

Fig. 30. Photograph showing Schottky diode, bisected pillbox dipole, and twisted-pair leads before assembly.

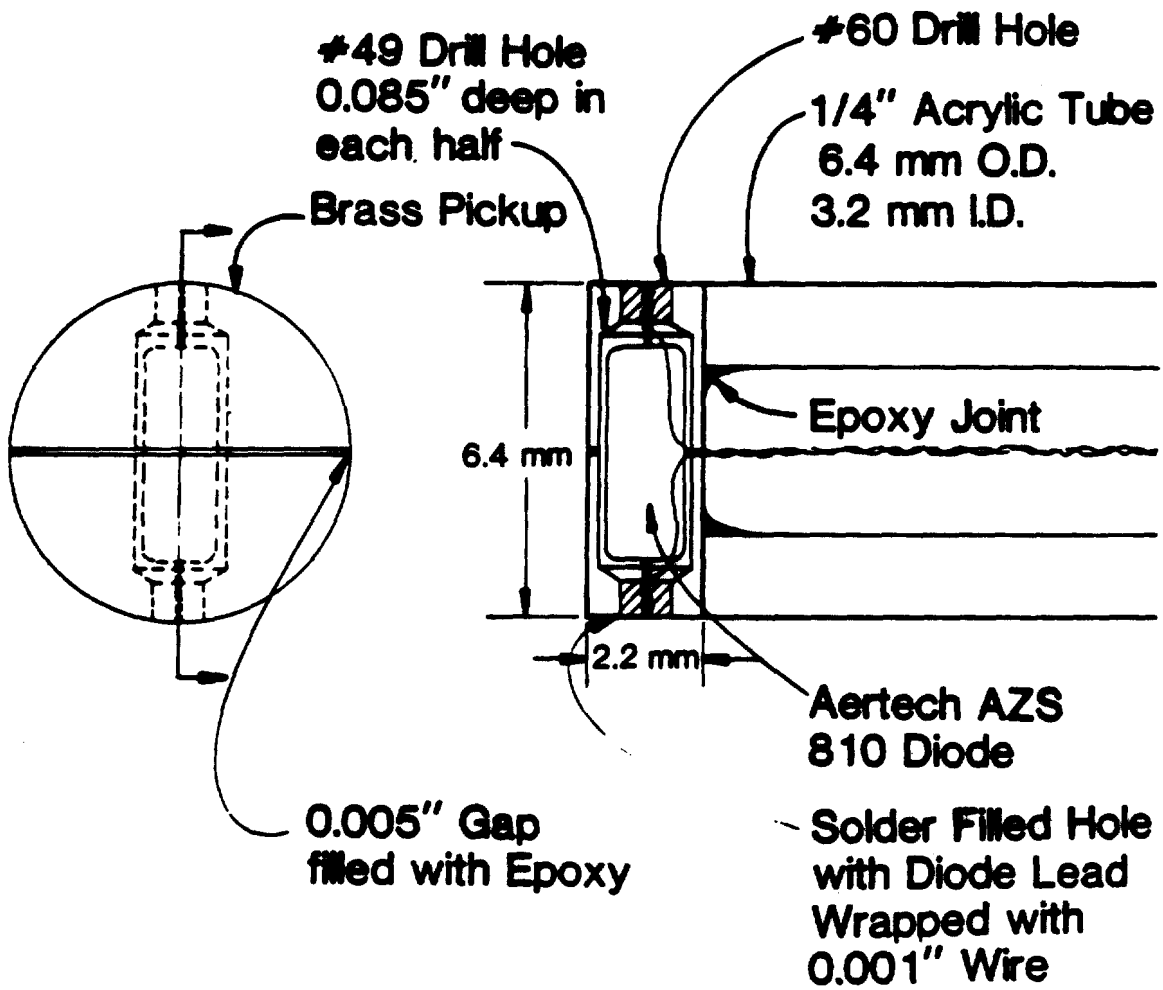

DIODE RF FIELD SENSOR

Fig. 31. Schematic of construction of diode probe for measuring electric-field strength.

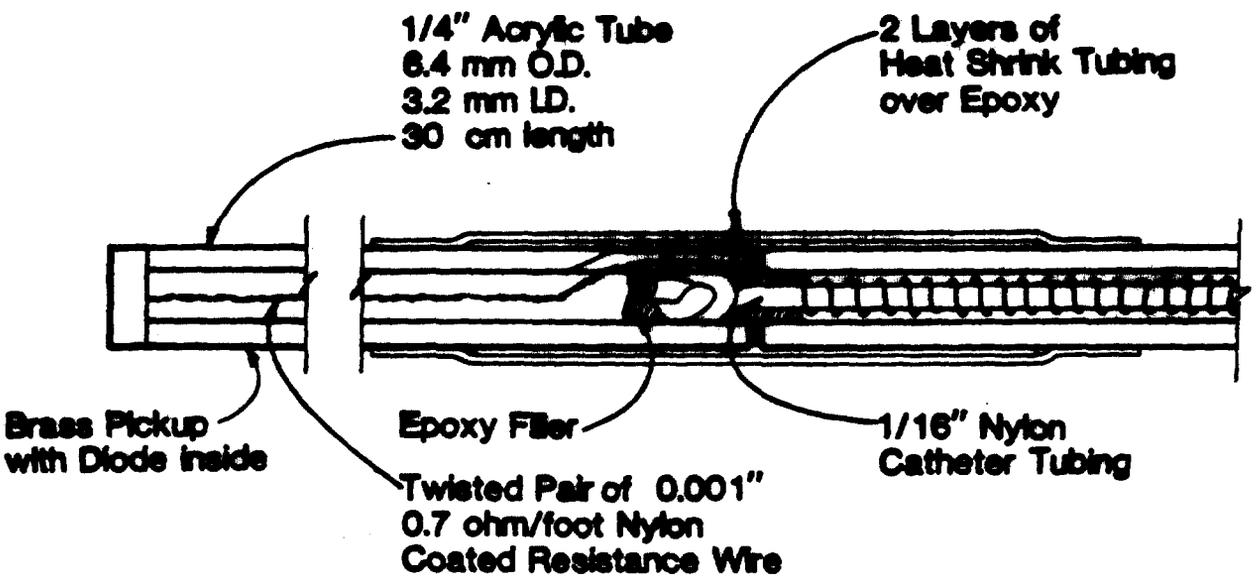

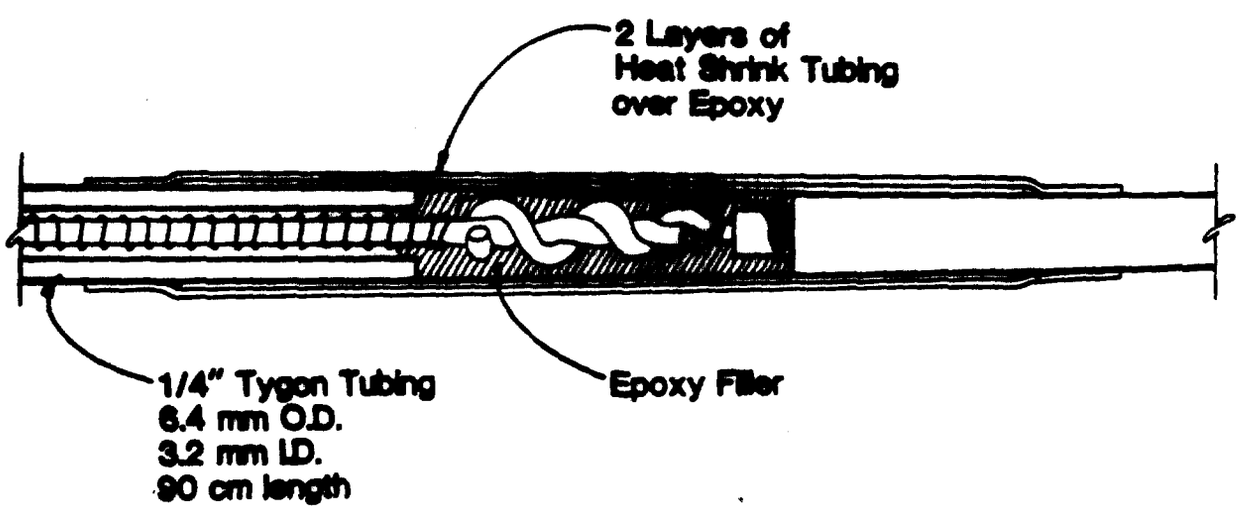

Fig. 31. (continued) Schematic of construction of diode probe for measuring electric-field strength.

leads were wrapped spirally around a 1/16" nylon catheter tube to take up any mechanical strain resulting from tension on the small twisted leads. At the end of the tygon tubing the twisted leads were connected to a standard RG58 shielded cable, which in turn was connected to the HP 415E standing wave detector, as shown in Fig. 32.

The diode sensor was calibrated with equipment shown in Fig. 33. A waveguide with 24.8- x 12.4-cm cross section was loaded with a 11.6-cm-thick section of phantom muscle tissue. The tissue was matched to the impedance of the waveguide with a quarter-wavelength section of Eccofoam HiK dielectric material (Emerson & Cuming Inc., K=6). The thickness of the dielectric slab was trimmed to 4 cm for a minimum VSWR of 1.33. The strength of the electric field and SAR at any point in the waveguide per watt input to the waveguide with width a and height b may be calculated as follows:

The power density, P, at any point in the waveguide as a function of z in the direction of propagation and the distance x from a side wall is

$$P = \mathrm{Re}\left[(E_0^2/4Z)e^{-2\alpha z}\sin\frac{2\pi x}{a}\right]$$

where $\alpha = \mathrm{Re}[\gamma]$

$$\gamma = j\frac{2\pi}{\lambda}S$$

$$S = \sqrt{\varepsilon - \left(\frac{\lambda}{2a}\right)^2}$$

$$Z = 120\pi/S$$

ε is the complex dielectric constant of the synthetic tissue, λ is the wavelength, and E_0 is the (rms) electric field strength at the surface of the synthetic tissue (z=0).

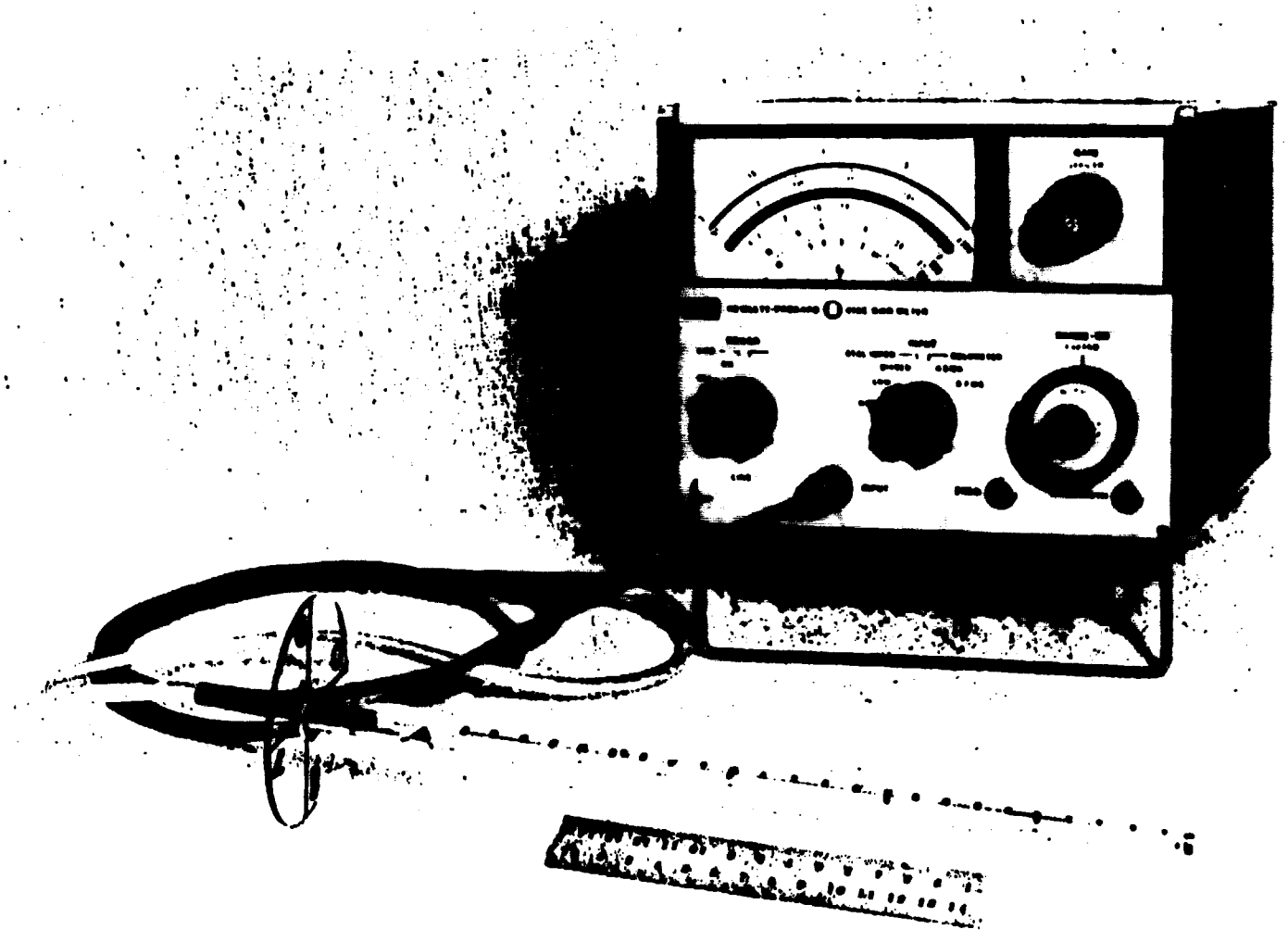

Fig. 32. Photograph of diode for measuring electric-field strength, cable, and HP 415E meter.

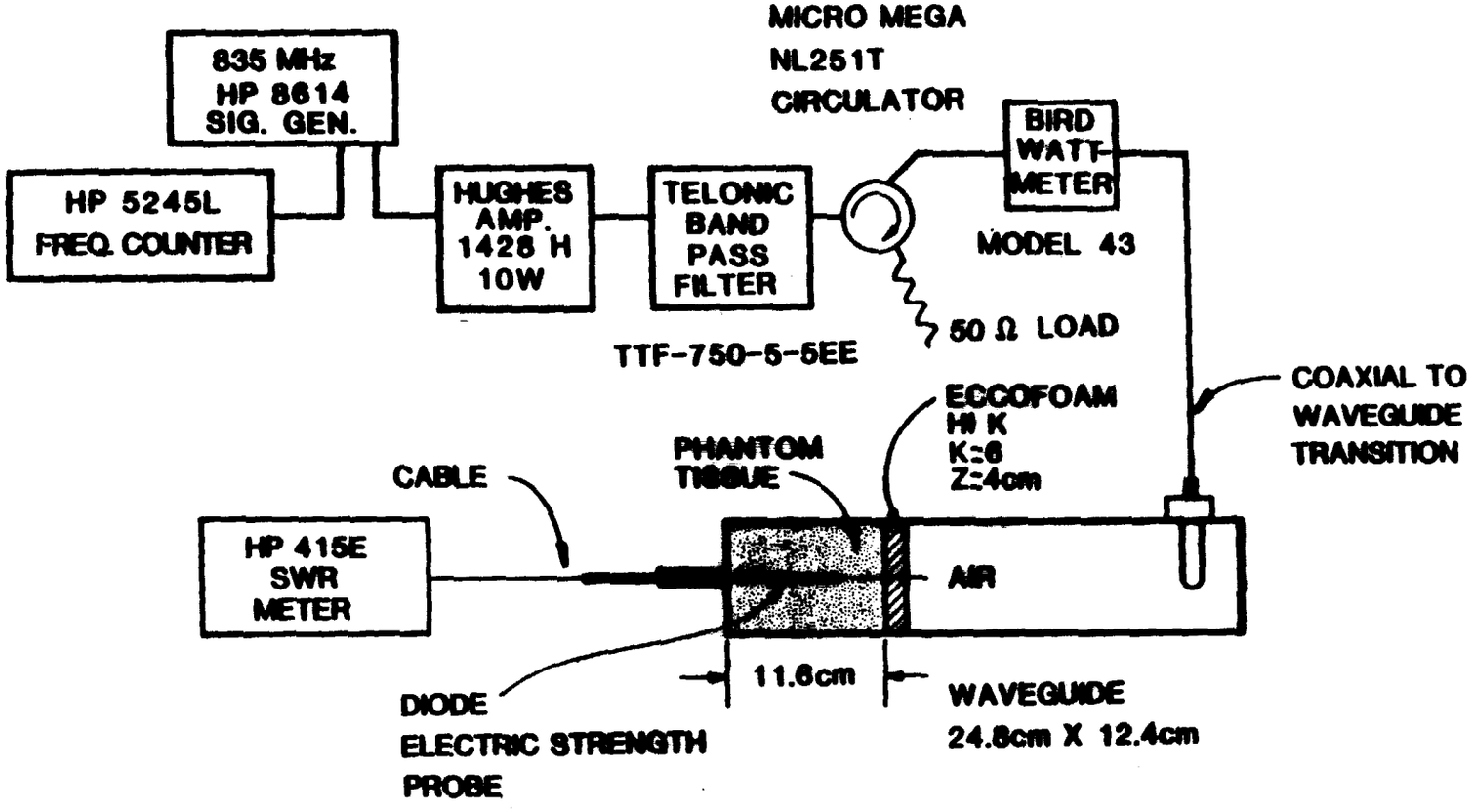

Fig. 33. Block diagram of equipment used for calibration of probe for measuring electric-field strength.

If we assume negligible loss up to the point z=0, the total input power is

$$P_{in} = \int_A P da = (ab/2) P e^{-2\alpha z},$$

or, in terms of input power,

$$P = 2(P_{in}/ab) e^{-2\alpha z},$$

$$E^2 = [240\pi \; P_{in}/abRe(S)] \; e^{-2\alpha z} \sin^2(\pi x/a).$$

The "apparent" power density, P_a, in mW/cm^2 as measured by field survey meter is

$$P_a = E^2/1200\pi,$$

and the SAR in W/kg is

$$SAR = 10^{-3}(\sigma/\rho)E^2.$$

The field strength and SAR along the axis of the waveguide, which varied with the depth from the muscle Eccofoam slab interface, are given in Table 3.

TABLE 3b. VALUES FOR ELECTRIC FIELD STRENGTH, APPARENT POWER DENSITY, ACTUAL POWER DENSITY AND SAR ALONG AXIS OF WAVEGUIDE AS FUNCTION OF DISTANCE FROM MUSCLE ECCOFOAM SLAB INTERFACE, WAVEGUIDE WITH DIMENSIONS 12.4 CM BY 24.68 CM, WITH 1-W INPUT POWER

DIELECTRIC CONSTANT OF MUSCLE = 50.6 -j.266

DISTANCE (CM)	ELECTRIC FIELD (V/m)	APPARENT POWER DENSITY (mW/cm2)	ACTUAL POWER DENSITY (mW/cm2)	SAR (W/kg)
0	5.807E+01	8.944E-01	6.535E+00	4.167E+00
1	4.223E+01	4.730E-01	3.456E+00	2.204E+00
2	3.071E+01	2.502E-01	1.828E+00	1.165E+00
3	2.233E+01	1.323E-01	9.667E-01	6.164E-01
4	1.624E+01	6.997E-02	5.112E-01	3.260E-01
5	1.181E+01	3.700E-02	2.704E-01	1.724E-01
6	8.589E+00	1.957E-02	1.430E-01	9.117E-02
7	6.246E+00	1.035E-02	7.562E-02	4.822E-02
8	4.542E+00	5.473E-03	3.999E-02	2.550E-02
9	3.303E+00	2.895E-03	2.115E-02	1.349E-02
10	2.402E+00	1.531E-03	1.119E-02	7.132E-03
11	1.747E+00	8.096E-04	5.916E-03	3.772E-03
12	1.270E+00	4.282E-04	3.128E-03	1.995E-03
13	9.239E-01	2.264E-04	1.655E-03	1.055E-03
14	6.719E-01	1.198E-04	8.750E-04	5.579E-04
15	4.886E-01	6.333E-05	4.628E-04	2.951E-04
16	3.553E-01	3.349E-05	2.447E-04	1.560E-04
17	2.584E-01	1.771E-05	1.294E-04	8.252E-05
18	1.879E-01	9.368E-06	6.845E-05	4.364E-05
19	1.367E-01	4.954E-06	3.620E-05	2.308E-05
20	9.939E-02	2.620E-06	1.914E-05	1.221E-05
VALUES FOR AIR FILLED GUIDE				
0	1.896E+02	9.531E+00	6.535E+00	0.000E-01

TABLE 3a. VALUES FOR ELECTRIC FIELD STRENGTH, APPARENT POWER DENSITY, ACTUAL POWER DENSITY AND SAR ALONG AXIS OF WAVEGUIDE AS FUNCTION OF DISTANCE FROM MUSCLE ECCOFOAM SLAB INTERFACE, WAVEGUIDE WITH DIMENSIONS 12.4 CM BY 24.68 CM, WITH 1-W INPUT POWER

DIELECTRIC CONSTANT OF MUSCLE = 50.6 -j.266

DISTANCE (mm)	ELECTRIC FIELD (V/m)	APPARENT POWER DENSITY (mW/cm2)	ACTUAL POWER DENSITY (mW/cm2)	SAR (W/kg)
0	5.807E+01	8.944E-01	6.535E+00	4.167E+00
1	5.625E+01	8.392E-01	6.132E+00	3.910E+00
2	5.448E+01	7.874E-01	5.753E+00	3.669E+00
3	5.278E+01	7.388E-01	5.398E+00	3.442E+00
4	5.112E+01	6.932E-01	5.065E+00	3.230E+00
5	4.952E+01	6.504E-01	4.753E+00	3.030E+00
6	4.797E+01	6.103E-01	4.459E+00	2.843E+00
7	4.646E+01	5.726E-01	4.184E+00	2.668E+00
8	4.501E+01	5.373E-01	3.926E+00	2.503E+00
9	4.360E+01	5.041E-01	3.684E+00	2.349E+00
10	4.223E+01	4.730E-01	3.456E+00	2.204E+00
11	4.090E+01	4.438E-01	3.243E+00	2.068E+00
12	3.962E+01	4.164E-01	3.043E+00	1.940E+00
13	3.838E+01	3.907E-01	2.855E+00	1.820E+00
14	3.718E+01	3.666E-01	2.679E+00	1.708E+00
15	3.601E+01	3.440E-01	2.513E+00	1.603E+00
16	3.488E+01	3.228E-01	2.358E+00	1.504E+00
17	3.379E+01	3.028E-01	2.213E+00	1.411E+00
18	3.273E+01	2.842E-01	2.076E+00	1.324E+00
19	3.170E+01	2.666E-01	1.948E+00	1.242E+00
20	3.071E+01	2.502E-01	1.828E+00	1.165E+00
VALUES FOR AIR FILLED GUIDE				
0	1.896E+02	9.531E+00	6.535E+00	0.000E-01

3 EXPERIMENTAL RESULTS

Field Mapping

Two meters were available for carrying out the mapping of the electromagnetic fields both inside and outside of the automobile. The NBS EDM-1C meter is most sensitive, with capabilities of measuring below 10 $\mu W/cm^2$, but is not calibrated for 835-MHz. Therefore, it was compared to a Holaday isotropic-broadband meter (Model HI 3001) from Bell Laboratories. It was found that if a correction factor of 1.83 was applied to the reading of the EDM-1C, it agreed very well with the Holaday meter at distances away from the source where there was no source-meter interaction. Since the Holaday meter has a larger sensor, the meter-source interaction was greater for it. Comparison of the measurements by the two meters (with corrected values for the EDM-1C meter) are shown in Table 4. In Figs. 34-37 are illustrated the measurements with respect to the roof-mounted antenna and the position of the exposed subjects. The measurements were made without the presence of the exposed subject. In Figs. 38-40 are illustrated the power-density measurements exterior to the automobile of the 835-MHz radiation from the trunk-mounted antennas with 1-W input.

Maximum exposure levels for the roof-mounted antenna varied from 64 $\mu W/cm^2$-per-watt input for the woman to 148 $\mu W/cm^2$-per-watt input for the child. Maximum exposure levels for the trunk-mounted antenna varied from 357 $\mu W/cm^2$-per-watt input for the child to 624 $\mu W/cm^2$-per-watt input for the woman.

The electromagnetic fields within the automobile were measured over a three-dimensional space where the upper body of the exposed subjects could be exposed to the radiation from the trunk-mounted antennas through the rear window of the car. The region over which the measurements were made every 10 cm in three directions is shown in Figs. 41 and 42. The coordinate system was arbitrarily chosen with the origin as shown in the figures. For the simulated exposures, the subjects were placed in positions where maximum fields were measured. Their relative positions in

TABLE 4. COMPARISON OF MEASUREMENTS OF POWER DENSITY (mW/cm^2) MADE WITH NBS EDM-1C AND HOLADAY 3001 SURVEY METERS AT 835-MHz, WITH 1-W INPUT TO SOURCE

Waveguide Open Aperture Source

Distance from source (cms)	0	5	10	15	20	25	30	40	50
NBS meter	11.82	5.68	2.64	1.44	0.859	0.514	0.374	0.186	0.136
Holaday meter	6.77	3.76	1.97	1.13	0.713	0.483	0.340	0.208	0.134

Roof-Mounted Antenna

Distance from source (cm)	35	45	55	57.5	60	70	80	90
NBS meter	0.141	0.095	0.083	0.084	0.075	0.046	0.046	0.037
Holaday meter	0.159	0.127	0.090	0.093	0.093	0.037	0.044	0.034

Trunk-Mounted Antenna Exterior of Automobile

Distance from source (cm)	15	25	35	45
NBS meter	0.456	0.196	0.091	0.069
Holaday meter	0.444	0.197	0.095	0.056

Trunk-Mounted Antenna Interior of Automobile

Distance from source (cm)	55	60	65	70	74	80
NBS meter	0.042	0.047	0.045	0.038	0.033	0.037
Holaday 3001 meter	0.035	0.047	0.045	0.039	0.032	0.028

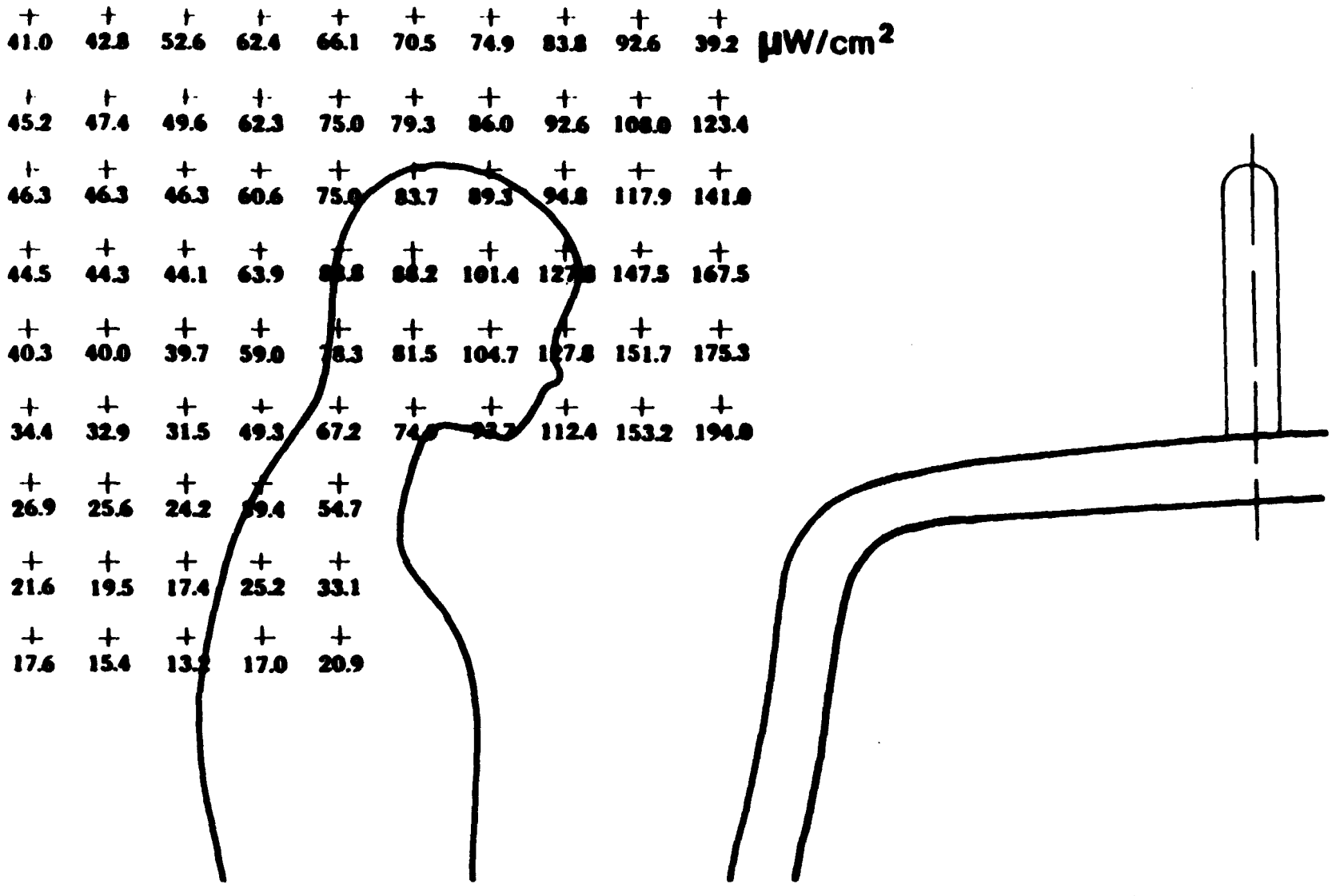

Fig. 34. Power densities exterior of automobile due to 835-MHz radiation from roof-mounted antenna, with 1-W input power (outline shows position of exposed woman model standing 43.5 cm from antenna).

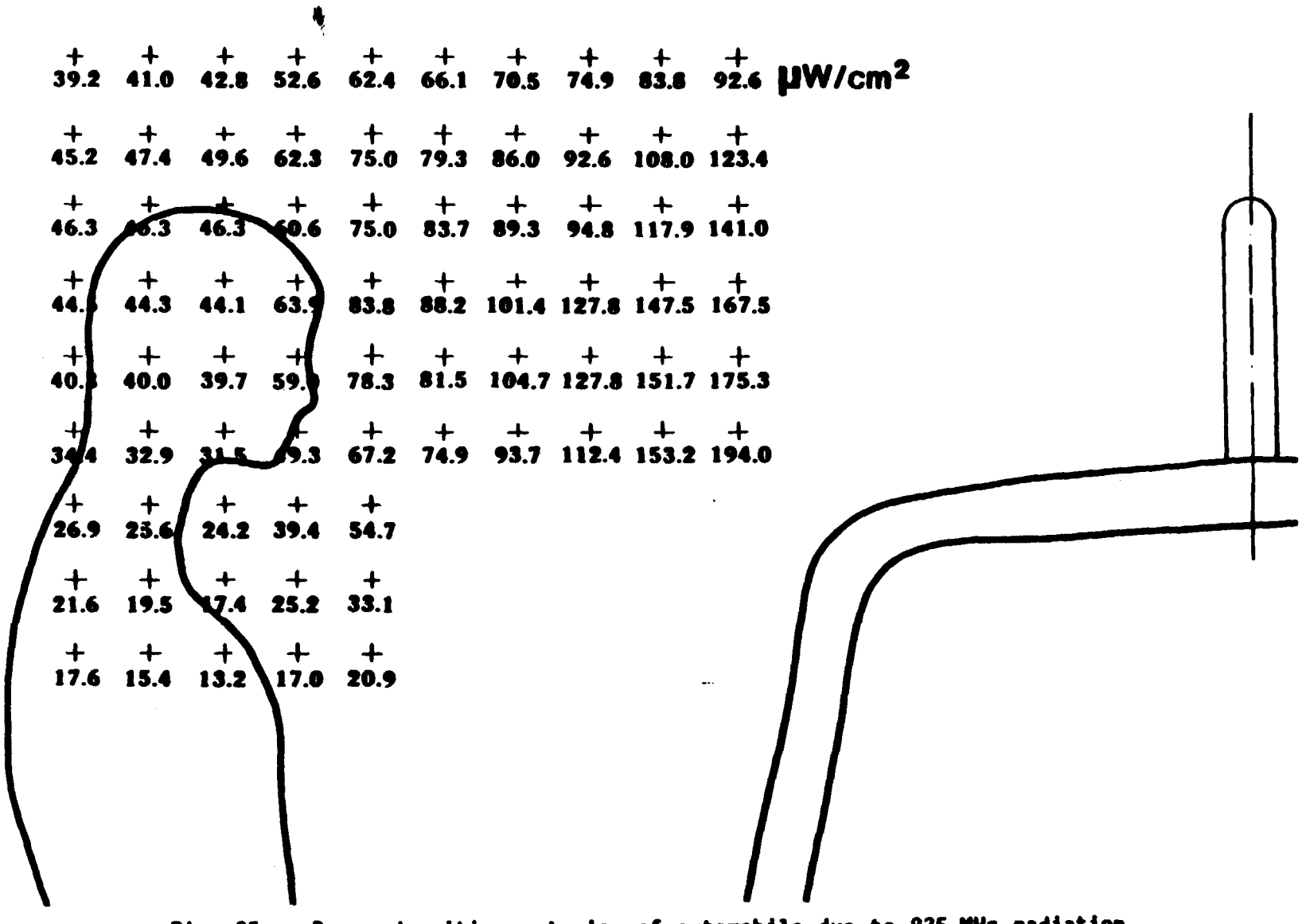

Fig. 35. Power densities exterior of automobile due to 835-MHz radiation from roof-mounted antenna, with 1-W input power (outline shows position of exposed woman model standing 63 cm from antenna).

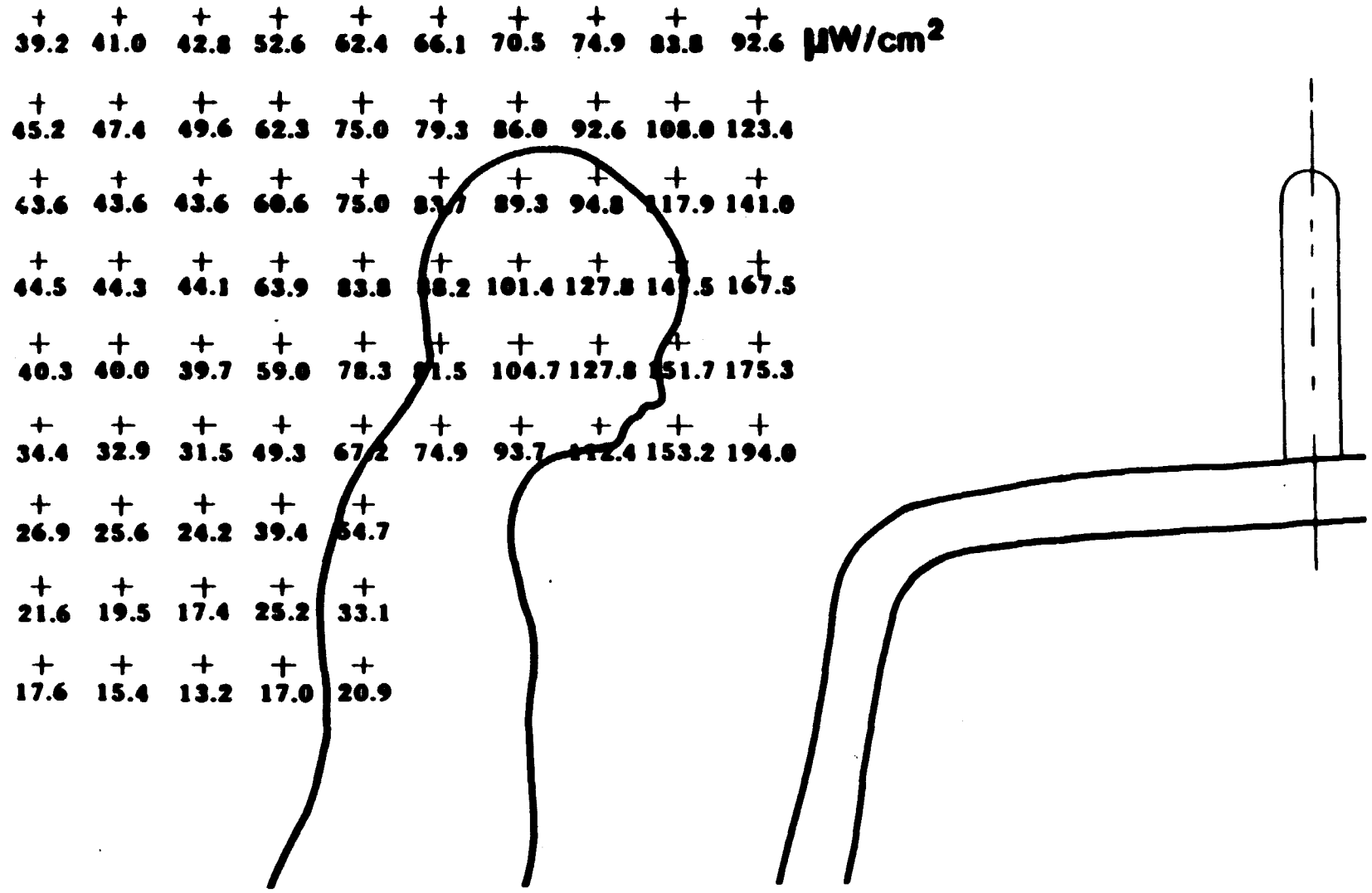

Fig. 36. Power densities exterior of automobile due to 835-MHz radiation from roof-mounted antenna, with 1-W input power (outline shows position of exposed child model held 39 cm from antenna).